Small angle X-ray scattering studies on transition metals nanoparticles

V. REDNIC[a], M. RADA[a], S. RADA[a], R. – C. SUCIU[a*], WU ZHONGHUA[b], XING XUEQING[b], F. MATEI[c], N. ALDEA[a]
[a] *National Institute for R&D of Isotopic and Molecular Technologies, Cluj-Napoca, 400293, Romania*
[b] *Beijing Synchrotron Radiation Facilities of Beijing Electron Positron Collider National Laboratory, Beijing, People's Republic of China*
[c] *University of Agricultural Sciences and Veterinary Medicine, Cluj-Napoca, 400372, Romania*

SAXS technique was used to examine the nanoparticle size and their shapes of supported gold catalysts. The experimental data are characterized by two main features as Guinier and Porod regions. The standard plots of the experimental data are available to fit the SAXS patterns to obtain the radius of gyration and the Porod exponent. A more elaborated Guinier and Porod empirical model is used to fit SAXS data from spherical as well as non spherical objects such as rods or platelets. It is also applied to shapes intermediate between spheres rods or between rods and platelets. The deconvolution method for nanoparticle sphere shape determination is developed. The experimental data were collected at Beijing Electron Positron Collider National Laboratory on 1W2A line operating at a wavelength of *1.54 Å*, distance between sample holder and CCD detector was *1.572 m*.

(Received July 20, 2015; accepted September 29, 2016)

Keywords: Grain size, SAXS, Guinier radius, Porod parameter, Nanoparticles shape

1. Introduction

The small angle X-ray scattering (SAXS) is one of the fields that has been rather recently opened. The study of SAXS was introduced when it became desirable to detect large lattice spacing of order of tens or hundreds of interatomic distances. These size spacing are found in some particular minerals and in certain complex molecules such as the high polymers or proteins [1]. If a sample has a non periodic structure or if its lattice has been sufficiently perturbed the diffraction patterns are not limited to spots, points or lines but contain more or less extended regions of scattering. Generally speaking SAXS technique is a non-destructive method and it consists in elastic scattering of X ray with wavelength around 1 up 2 *Å* by a sample which has inhomogeneities in the *Å*-range, and it is recorded at very low angles typically 0.1 - 5°. The scattered X-rays form a scattering pattern is then recorded at a detector which is typically a 2-dimensional flat and it is situated behind the sample perpendicular to the direction of the primary beam that initially hits the sample. Interference patterns of objects vary along with the nature of the samples including the symmetry of matrix of molecules embedded and the freedom of molecules inside of the matrix.

Fig. 1 illustrates the sample states and interference patterns. The 2D images have been converted in ASCI data by using FIT2D computer code [2]. The software is available free of charge at htttp://www.esrf.fr/computing/scientific/FIT2D/. A new Guinier–Porod empirical model is introduced. The SAXS experimental data of supported gold catalysts are analyzed either using standard Guinier or Porod analysys [3] or using our own methods to find the best Guinier radius of gyration, Porod exponent and probability distribution function of the grain size. The standard method is easily performed and usually gives good estimations of particle size. Porod parameter furnishes information regarding the nature of the scattering inhomogeneities such as [3]: if exponent d = 4 points to particles with smooth surfaces while d = 3 points to very rough surfaces. An exponent d = 3 can also point to scattering from 'collapsed' polymer chains (in a bad solvent) and d = 5/3 points to scattering from 'fully swollen' chains (in a good solvent). An exponent d = 2 can represent scattering either from Gaussian polymer chains or from a two-dimensional structure (such as lamellae or platelets). An exponent d = 1 represents scattering from a stiff rod (or thin cylinder). Porod exponents less than 3 are for 'mass fractals' while Porod exponents between 3 and 4 are for 'surface fractals'.

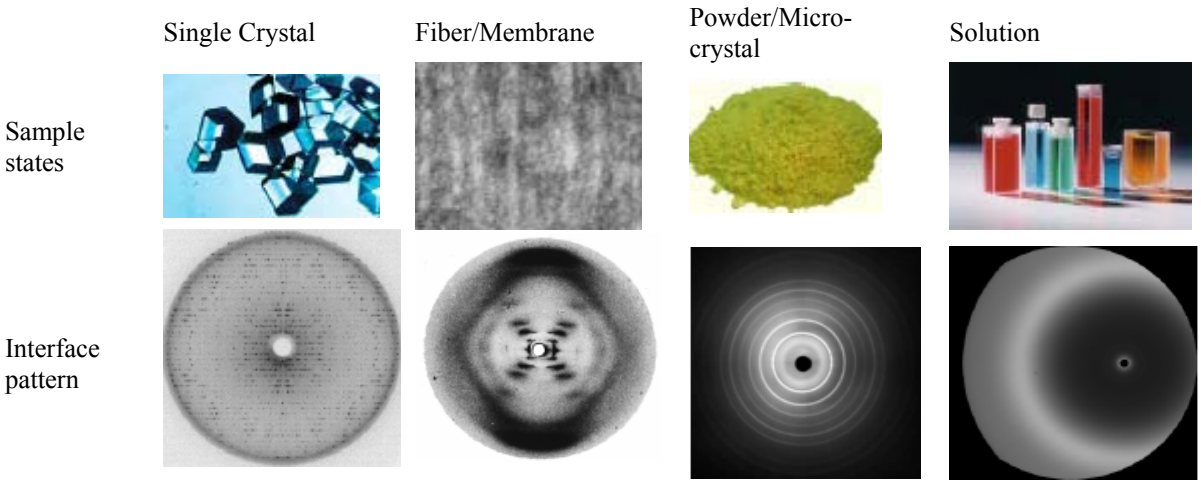

Fig. 1: Images of SAXS interference patterns for different type of samples

2. Theoretical background and samples preparation

By theoretical considerations [1] the scattered intensity versus momentum transfer given by $q=4\pi \sin(\theta)/\lambda$ could be expressed by two distinctly regions. The scattered intensity for the first domain when $q \to 0$ named Guinier region can be given by relation:

$$I_G(q) = G\, e^{-\frac{R_G^2 q^2}{3}} \tag{1}$$

while the second region with higher q values, scattered intensity can be approximated by:

$$I_P(q) = \frac{D}{q^d} \tag{2}$$

where parameters R_G, d are Guinier radius and Porod exponent, respectively. D and G are constants for the investigated range and are determined by fit techniques.
Limit borders of both regions can be determined from mathematical consideration by finding a q_0 value with requirement that the values of the Guinier and Porod terms and their derivatives to be continuous at the q_0 value, thus the following relationships between parameters are obtained:

$$q_0 = \frac{1}{R_G}\sqrt{\frac{3d}{2}} \tag{3}$$

$$D = q_0 G\, e^{-\frac{q_0^2 R_G^2}{3}} = \frac{G}{R_G^d}\sqrt{\left(\frac{3d}{2}\right)^d}\, e^{-\frac{d}{2}}$$

The scattered intensity can also be analyzed in terms of the scattering factors. There are presented the analytical particularly scattering factors relations based on particles of different shapes such as: sphere of radius R, ellipsoid of revolution, cylinders of revolution, rod of infinitesimal transverse dimensions, or flat disc of infinitesimal thickness [1]. For the sphere shape, which is the simplest one, the scattering factor is given by:

$$F(q) = 3\frac{\sin qR - qR\cos qR}{(qR)^3} \tag{4}$$

From statistically point of view the scattered intensity can be describe in terms of following relation:

$$I(q, p_1, p_2 \ldots) = N \int_{R_{\min}}^{R_{\max}} F^2(q,R)\; p(R, p_1, p_2 \ldots) dR \tag{5}$$

where N, R_{min}, R_{max}, $p(R,p1,p2,...)$ represent the normalization factor, minimum and maximum values of spheres radius and the probability distribution function of nanoparticles, respectively.

Supported gold catalysts were prepared by homogeneous deposition–precipitation with urea on support of MO_x/Al_2O_3 (M: Zn, Mg, Ce, Zn and Ti in different combinations) [4]. The gold precursor was $HAuCl_4 3H_2O$, Aldrich, 99.999% purity. The theoretical gold content for the catalysts was around 5 wt%. The catalysts were calcinated at 300 °C before measurements.

3. Results and discussion

The experimental SAXS spectra, obtained after application of fit2D program, for $Au/ZnO/MgO/Al_2O_3$, $Au/CeO_x/ZrO_x/Al_2O_3$ and Au/TiO_2 are given in figure 2.

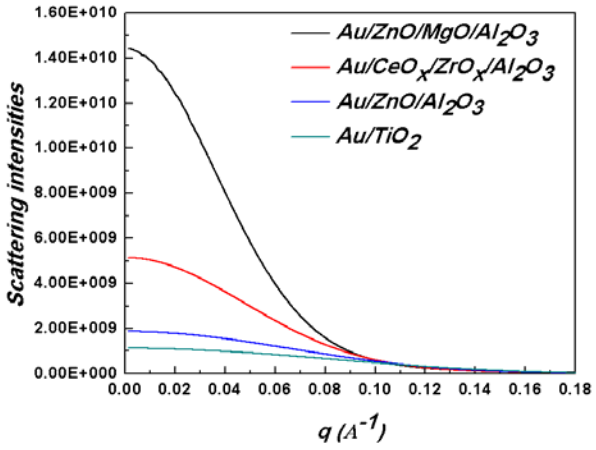

Fig. 2: SAXS experimental data of the investigated samples

The first step of data analysis consists in X ray scattering intensities were normalized against incident I_o. In the next step the extraction of SAXS signal is based on the determination of background correction due to both inelastic scattering and fluorescence X-ray contribution to scattering processes. They do not interfere with elastically scattering X-ray due to their different wavelengths. Practically it is realized by subtracting a polynomial curve obtained by fitting the first and the last a few tens of data. After the background removal the data are approximated with 3rd order bell spline functions [5] to ensure a good continuity. Initial determination of the Guinier and Porod regions is expressed by a trial q_0 value which is defined by the Gaussian dispersion of the data. Then q_0 values is shifted by using a statistical scenario defined by user and for each step the parameters from eqs. 1-2 and their standard deviation are stored in a temporally file. The best q_0 value is furnished by the minimum value of the standard deviation and its validity is verified by relation (3) accepting a certain errors limit. The results of this procedure for $Au/CeO_x/ZrO_x/Al_2O_3$ and Au/TiO_2 systems are graphical illustrated in figure 3. The calculations were done in the hypothesis of monodisperse samples.

Beside Guiner and Porod analysis of experimental data we developed a procedure for a large variety of the probability distribution function determination by taking into account a spherical shape of nanoparticles. This procedure is based on the analytical expression of scattering intensity furnished by relation 5. This is based on assumption that we have a set of N data points: (q_i, $I(exp)_i$) and the function $I(q;p1,p2...\ p_m)$ of known analytical form. It is worth to note that the function depends on the independent variable q, as well as on m parameters p_1 to p_m. Fitting this function to the data means finding those (p_1, p_2..., p_m) values that optimize a certain merit function, which represents a function measuring how well the data is represented by the function. The most common merit function is the minimum sum of the deviations squares given by

$$\min\left(\sum_{i=1}^{Np}\left(I_i(q_i,p_1,p_2\cdots p_m)-I_i(\exp)\right)^2\right).$$

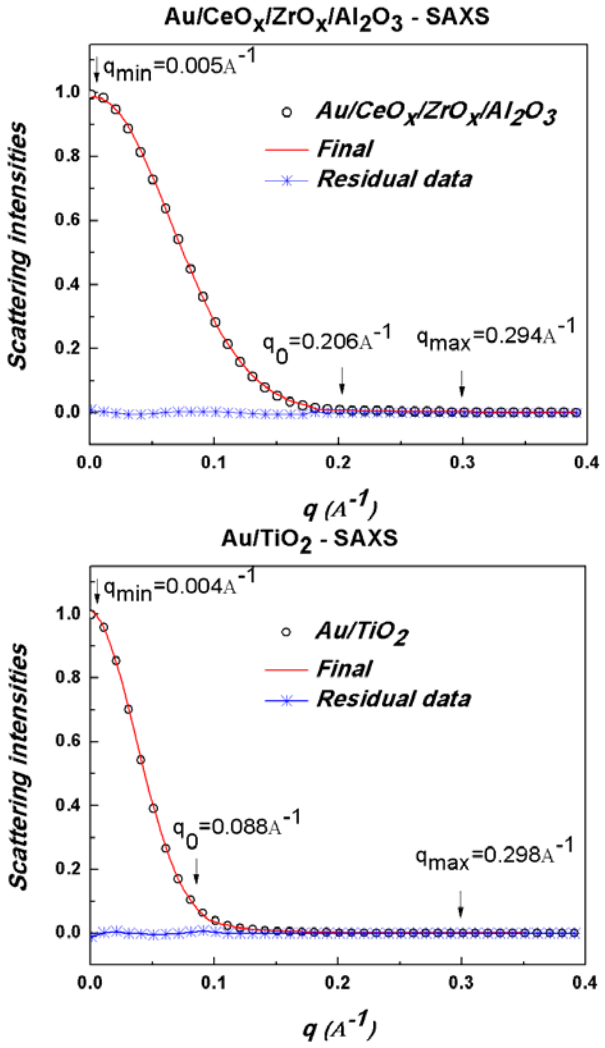

Fig. 3: SAXS data for $Au/CeO_x/ZrO_x/Al_2O_3$ and Au/TiO_2 together with the fit to the Guinier–Porod model eqs (1-2); d= 2.203 - lamellae or platelets structure (up) and d= 3.97 - particles with smooth surfaces (down); The fitting region is delimited by arrows.

The best parameters p_1, p_2,... p_m situated inside of integrals are determined by Levenberg and Marquard algorithm [7]. Figure 4 illustrates the trial solutions and Fig. 5 the final solution obtained after implementation of the procedure.

The Table 1 contains numerical results. The second up forth columns contain the q_{min}, q_0 and q_{max} values. The fits were performed in the q range from q_{min} to q_{max}. The q_0 that is the border between the two regions was determined like our scenario described above and together with the extreme values were marked in figure 3 by vertical arrows. The fifth and sixth columns present numerical values and their uncertainties of the Gunier radius and shape Porod parameters.

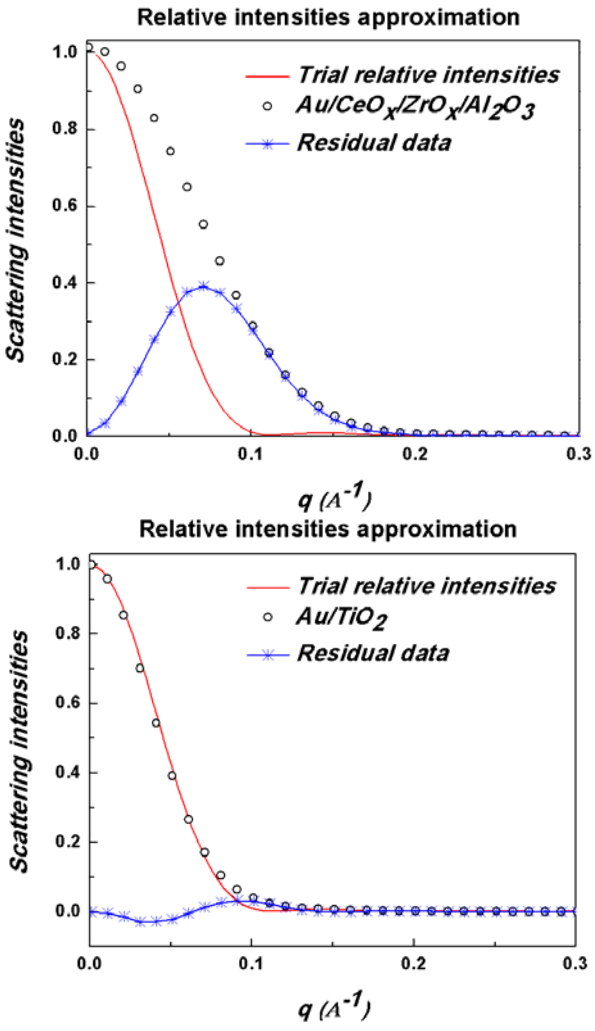

Fig. 4: Calculation the scattering intensities for Au/CeOx/ZrOx/Al_2O_3 (up) and Au/TiO_2 (down) systems using a trial parameters of probability distribution function.

It is important to mention from theoretical point of view that the particle size determined by SAXS is an averaging result based on preliminary consideration that all particles have orientation equally probable and it is not associated with any crystallographic plane. Porod parameter gives additional information regarding the global particle shape. Based on relation 5 the following three columns furnish structural parameters of investigated samples such as average radius, their uncertainties and standard deviation of normal probability distribution function. The last column gives the crystallite size associated to (111) crystallographic plane determined by Scherrer relation [6], obtained from XRD patterns investigation. Because the gold concentration from investigated samples is around than 5 wt% Au it is not possible to investigate other crystallographic plane so we couldn't do a realistic image regarding the crystallite shape. It only could be described by Porod parameter. The differences between the values of seventh (2*R) and the last column can be explained by distinction of the physical meaning of crystallite size, obtained by applying the Scherrer method to XRD patterns, and the grain size which is obtained using Guinier method on SAXS measurement. It is possible that a grain of gold nanocluster is built up from some more gold crystallites. Both data analysis are realized by own computer code developed in Gnuplot language and it shows intermediate processing results in a friendly graphic manner.

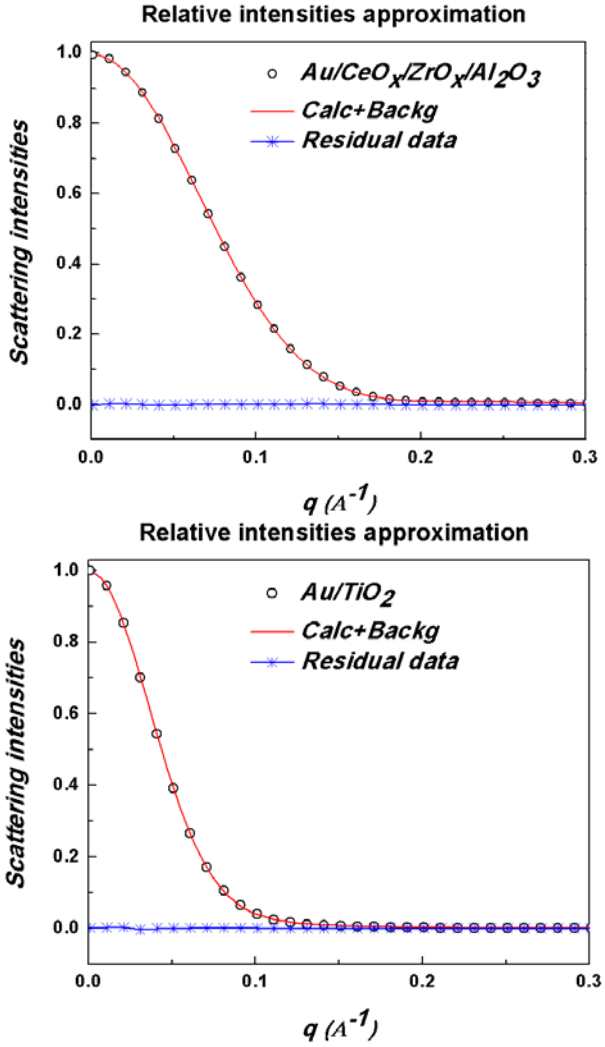

Fig. 5: The comparison between experimental and calculated data based on deconvolution technique for Au/CeOx/ZrOx/Al_2O_3 (up) and Au/TiO_2 (down) samples

4. Conclusions

In this contribution it was shown how to obtain structural information of supported gold catalysts based on SAXS measurement results using synchrotron radiation. The following conclusion can be drawn from these studies:

(i) A simple Guinier–Porod model described here can empirically model widely different;

Table 1: The structural parameters and their uncertainties for supported gold catalysts

Samples	Wavevector domain [Å^{-1}]			Guiner radius Rg±ΔRg [Å]	Porod parameter d±Δd	Spherical shape Normal distribution			Crystallite size by X-ray diffraction (Scherrer method) [Å]
	q_{min}	q_0	q_{max}			2*R [Å]	σ [Å]	Stdev	
$Au/ZnO/MgO/Al_2O_3$	0.0058	0.1620	0.2254	17.4 ±0.116	1.844±0.057	40.2	0.1	0.00242	25
$Au/CeO_x/ZrO_x/Al_2O_3$	0.0038	0.1627	0.2244	20 ±0.045	2.203±0.055	48.2	3.4	0.00130	30
$Au/ZnO/Al_2O_3$	0.0032	0.1304	0.2252	25.2 ±0.049	3.727±0.136	64.6	6.5	0.00092	42
Au/TiO_2	0.0017	0.0875	0.2274	31 ±0.122	3.97±0.053	83.4	9.3	0.00115	53

(i) structures and could provide a reliable procedure for obtaining useful information from the X ray scattering on a spherical or non spherical object;

(ii) A useful method was elaborated for many type of the probability distribution function determination for nanoparticles with spherical shape;

(iii) The particle size and shape of supported gold catalysts determined by SXAS can be correlated with the crystallite size calculated by X-ray diffraction analysis by taking into consideration the difference between grain and crystallite sizes;

(iv) The models adopted here for SAXS data analysis cannot reproduce oscillations characteristic of form factors for compact monodisperse scattering objects.

References

[1] A. Guinier, G. Fournet, Small-angle scattering of X-rays, John Wiley & Sons, New York (1955).
[2] A. P. Hammersley, S. O. Svensson, M. Hanfland, A. N. Fitch, D. Hausermann, High Pressure Res **14**, 235 (1996).
[3] B. Hammouda, J. Appl. Cryst. **43**, 716 (2010).
[4] R. Grisel, Kees-Jan Weststrate, A. Gluhoi, B. E. Nieuwenhuys, Gold Bulletin **35** (2), 39 (2002).
[5] N. Aldea, E. Indrea, Comput. Phys. Commun. **51**, 451 (1988).
[6] N. Aldea, V. Rednic, S. Pintea, P. Marginean, B. Barz, A. Gluhoi, B. E. Nieuwenhuys, M. Neuman, Xie Yaning, F. Matei, Superlattices Microst **46**, 141 (2009).
[7] D. Marquardt, JSIAM, **11**, 431 (1963).

*Corresponding author: Ramona.Suciu@itim-cj.ro